Pergamon

Bioorganic & Medicinal Chemistry, Vol. 5, No. 6, pp 1173–1184, 1997

PII: S0968-0896(97)00064-3
0968-0896/97 $17.00 + 0.00

Discovery of Selective, Small-Molecule Inhibitors of RNA Complexes—I. The Tat Protein/TAR RNA Complexes Required for HIV-1 Transcription

Houng-Yau Mei,[a,*] David P. Mack,[a,*] Adam A. Galan,[a] Nadia S. Halim,[a] Andrea Heldsinger,[d] Joseph A. Loo,[b] David W. Moreland,[c] Kristin A. Sannes-Lowery,[b] Lamia Sharmeen,[d] Hoa N. Truong[a] and Anthony W. Czarnik[a]

[a]BioOrganic Chemistry Section, [b]Analytical Research Section, [c]Biomolecular Structure and Drug Design Section, Department of Chemistry, and [d]Infectious Diseases Section, Department of Therapeutics, Parke-Davis Pharmaceutical Research, Division of Warner-Lambert Company, 2800 Plymouth Road, Ann Arbor, MI 48106, U.S.A.

Abstract—We have developed a therapeutic program focusing on the inhibition of a human immunodeficiency virus-1 specific protein–RNA interaction. This program begins with a search for small organic molecules that would interfere with the binding of Tat protein to TAR RNA. The methodologies chosen to study the HIV-1 Tat–TAR interaction and inhibition include gel mobility shift assays, scintillation proximity assays, filtration assays, and mass spectrometry. These methods helped establish in vitro high-throughput screening assays which rapidly identified Tat–TAR inhibitors from our corporate compound library. Tat-activated reporter gene assays were then used to investigate the cellular activities of the Tat–TAR inhibitors. The cellular activity, selectivity, and toxicity data for select Tat–TAR inhibitors were determined. Evaluation of both the cellular data and the Tat–TAR inhibition results led to further testing in anti-HIV-1 infection assays. © 1997 Elsevier Science Ltd.

Introduction

Transcription of human immunodeficiency virus (HIV-1) proviral DNA in infected cells proceeds through a complicated mechanism including a specific viral protein–RNA interaction.[1] The viral RNA genome contains a long terminal repeat domain (LTR) within which lies the transactivation response element (TAR) that is recognized by an HIV-1 regulatory protein, Tat.[2] In infected host cells, TAR has been suggested to recruit Tat and other cellular proteins to form a stable transcription complex with RNA polymerase II (Fig. 1). A direct correlation has been found between Tat binding to TAR RNA and the up-regulation of HIV-1 mRNA transcription.[3] Further evidence also suggests that interruption of the Tat–TAR interaction blocks HIV-1 replication in infected cells.[4]

Recent developments in combination therapy support a multi-target strategy for fighting HIV-1 infection.[5] There has been significant interest in finding therapeutics which target the HIV-1 Tat–TAR interaction. Amino acid or nucleotide-based analogues derived from Tat or TAR[6] and aminoglycoside antibiotics[7] interfere with the Tat–TAR interaction. Unfortunately, these molecules are unlikely to become viable anti-HIV-1 agents until either their low bioavailability or high toxicity is satisfactorily resolved. The cellular functions of Tat can be inhibited by small molecules such as benzodiazepines[8a] and epoxy steroids.[8b] However, mechanisms other than inhibiting Tat–TAR interaction have been suggested as responsible for their anti-viral activities.[9] Small-molecule intervention of Tat–TAR interaction remains to be explored.

Here we report a drug discovery approach beginning with a high-throughput screening strategy to identify compounds that inhibit the Tat–TAR interaction. Of course, because of the rarity of selective RNA small ligands, such inhibitors are of special significance. Inhibitors that block Tat binding to TAR are then chosen for more stringent testing in whole cell assays. These cellular assays utilize a reporter gene whose expression is activated by the Tat–TAR interaction.[10] The activity, selectivity, and toxicity of a Tat–TAR inhibitor can be determined using these cellular assays and appropriate controls. This approach allows us to identify high value leads that inhibit both Tat–TAR interaction and Tat-activated transcription in a cellular environment. These leads therefore constitute in vitro a significant first step in discovering drugs that intercept HIV-1 replication through a mechanism involving a unique protein–RNA interaction.

Results and Discussion

Tat, TAR and the Tat–TAR complex

'TAR', residues 1–59 of HIV-1 mRNA, adopts a unique hairpin–stem–bulge structure crucial for transactivation.[11] Figure 2(A) shows the 31-nucleotide RNA (TAR_{31}) used in our studies. TAR_{31} contains a portion

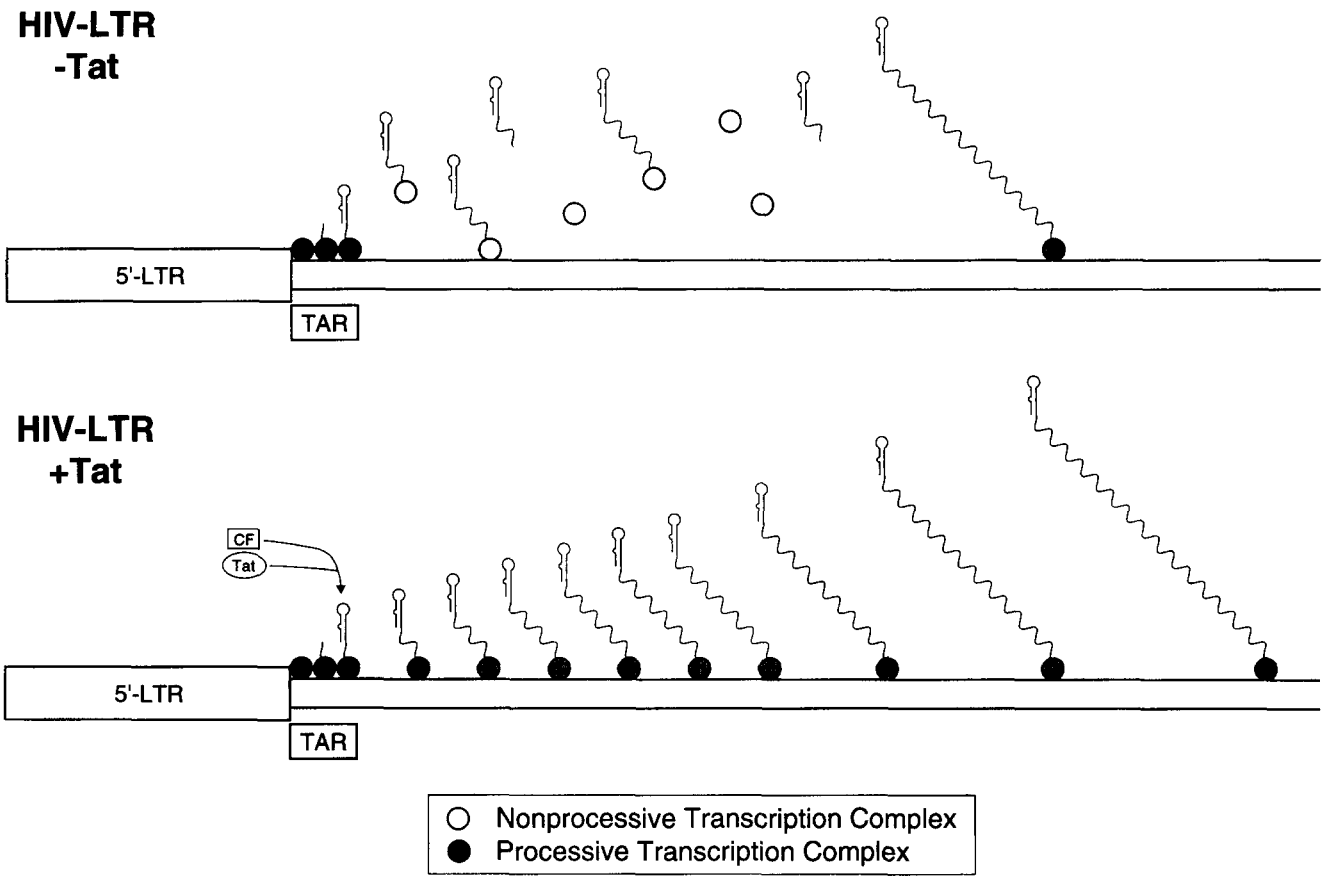

Figure 1. A model for Tat-transactivation in HIV-1. Tat facilitates transcription initiation/elongation. Top: in the absence of Tat, the transcriptional complex is nonprocessive. Only basal level of full-length transcripts was formed. Bottom: TAR in the LTR domain recruits Tat and some other cellular factors, the transcriptional complex is processive. The transcription of the full-length HIV-1 mRNA is activated up to several thousandfold.

of the full-length TAR RNA (residues 18–44) and has been shown to be sufficient for specific recognition by Tat.[12] Tat, an 86-amino acid HIV-1 specific protein, contains an arginine-rich basic domain (residues 47–58) involved in binding to TAR RNA.[13] Peptide fragments

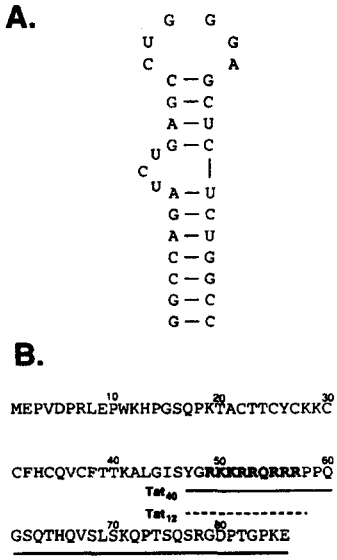

Figure 2. (A) The sequence of TAR RNA used in this study. (B) The sequence of Tat protein, Tat_{12} peptide (represented by - - - -), and Tat_{40} peptide (represented by ——). Highlighted area is the basic domain responsible for TAR RNA binding.

containing the basic domain of Tat share similar TAR binding characteristics with the wild-type protein.[14] Figure 2(B) shows a 12-amino acid peptide (Tat_{12}), a 40-amino acid peptide (Tat_{40}), and the full-length Tat protein used in our studies.

Mutagenesis analysis[2,14] and spectroscopic methods have been used to characterize the detailed mechanism of Tat–TAR interactions.[15] The UCU bulge and its neighboring base pairs in the upper stem domain of TAR have been postulated to make specific interactions with an arginine residue (52 or 53) of Tat. Compared to nonspecific arginine–RNA interactions, a 40-fold increase in binding affinity has been estimated for the arginine–RNA bulge interaction found in Tat–TAR complexes. NMR studies have shown, on complexation, conformational changes for both TAR RNA and Tat.[15]

Selected methods for studying HIV-1 Tat–TAR interaction

Methods such as mutagenesis and NMR spectroscopy can provide detailed information about the structure of free and complexed Tat or TAR. However, given the amount of time, material, and effort needed for these methods, they are unlikely to be useful in handling a large number of samples. To quickly identify inhibitors

of the Tat–TAR interaction from a large compound library, methods that are simple, sensitive, and amenable to high-throughput screening are required. To this end, we have employed a number of techniques—including gel mobility shift, scintillation proximity assay (SPA), filter binding assays, and electrospray ionization mass spectrometry (ESI-MS)—to study Tat–TAR interactions. Each of these techniques provides a different way to not only examine the Tat–TAR interaction, but also to study inhibitors of the system. The gel shift, SPA, and filter-binding assays are shown schematically in Figure 3. Each of these assays is based on the ability to distinguish the protein (peptide) or RNA from the complex. In the gel shift assay, free RNA is separated from the complex by electrophoresis. In the SPA method, free peptide is distinguished from the RNA-bound peptide on the bead surface. In the filter assay, free RNA is separated from complexed RNA by absorption of the protein or complex to the filter membrane.

The gel mobility shift assay has been widely used to study protein–nucleic acid interactions including the HIV-1 Tat–TAR interaction.[16] In this assay, ^{32}P-labeled free RNA is separated from the RNA–protein (peptide) complex by nondenaturing polyacrylamide gel electrophoresis due to differences in both the charge and mass of the two species. The protein (peptide)–RNA complex travels more slowly through the gel than does the free RNA, thus producing the mobility shift

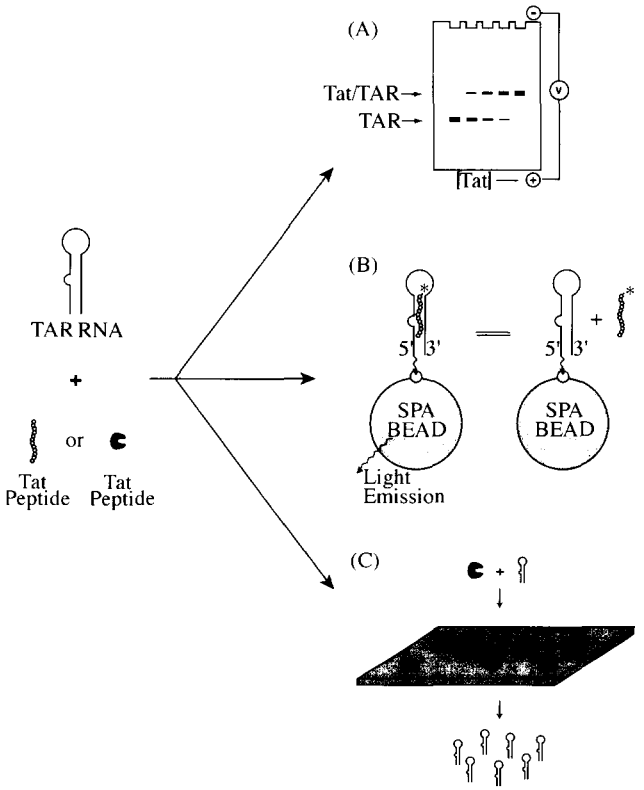

Figure 3. Methods used in studying Tat–TAR interaction. (A) Gel mobility shift assay. (B) Scintillation proximity assay. (C) Filtration assay.

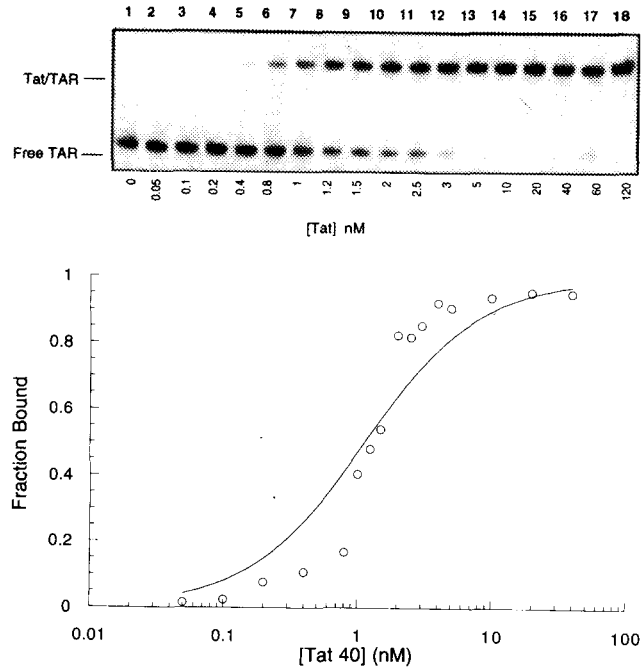

Figure 4. Gel mobility shift data of Tat_{40} binding to TAR_{31}. Top: Autoradiogram of a nondenaturing gel containing samples of free TAR_{31} and TAR_{31} samples titrated with increasing amount of Tat_{40}. Free TAR_{31} that migrates faster can be readily separated from the Tat_{40}–TAR_{31} complex. Bottom: Titration curve of the Tat_{40} binding to TAR_{31}. Data were obtained from gel mobility shift experiments such as the one described above. Data were fitted to the equation $\theta = [P]/[P] + K_d$, where θ is the fraction of RNA bound and [P] is the concentration of peptide. Since artifacts of the gel technique could affect the slope of the curve,[16] a hill coefficient of 1 (implied in the equation) was used to fit the data and should not affect the calculated value of K_d significantly.

(Fig. 3A). By varying the concentration of the protein (peptide) in the reaction over an appropriate range and quantitating the amount of free RNA vs bound RNA observed on the gel, a titration curve can be generated to provide a value for the apparent dissociation constant of the interaction (Figure 4). It has recently been shown that for very low dissociation constants (<1 nM), the gel shift technique overestimates the dissociation constant.[16] The value of K_d determined under these conditions is approximately 1 nM. Although this is likely to be an overestimation, it does not diminish the usefulness of this technique for examining other aspects of the system such as mutations and relative inhibition by competitors.

The scintillation proximity assay is a versatile assay that can be configured in many ways.[17] The basis of this technology is that scintillant is embedded in a solid bead that can be coated with a variety of proteins. Streptavidin-coated beads were used in these experiments. Given this configuration, these beads emit light when brought within close proximity of a radioisotope. Utilizing an appropriate radioisotope, ^{3}H or ^{125}I, involves choosing radioactive particles weak enough in energy such that when free in solution they are quenched prior to interacting with a bead. Thus, to study the interaction of Tat_{12} with TAR RNA, ^{125}I-

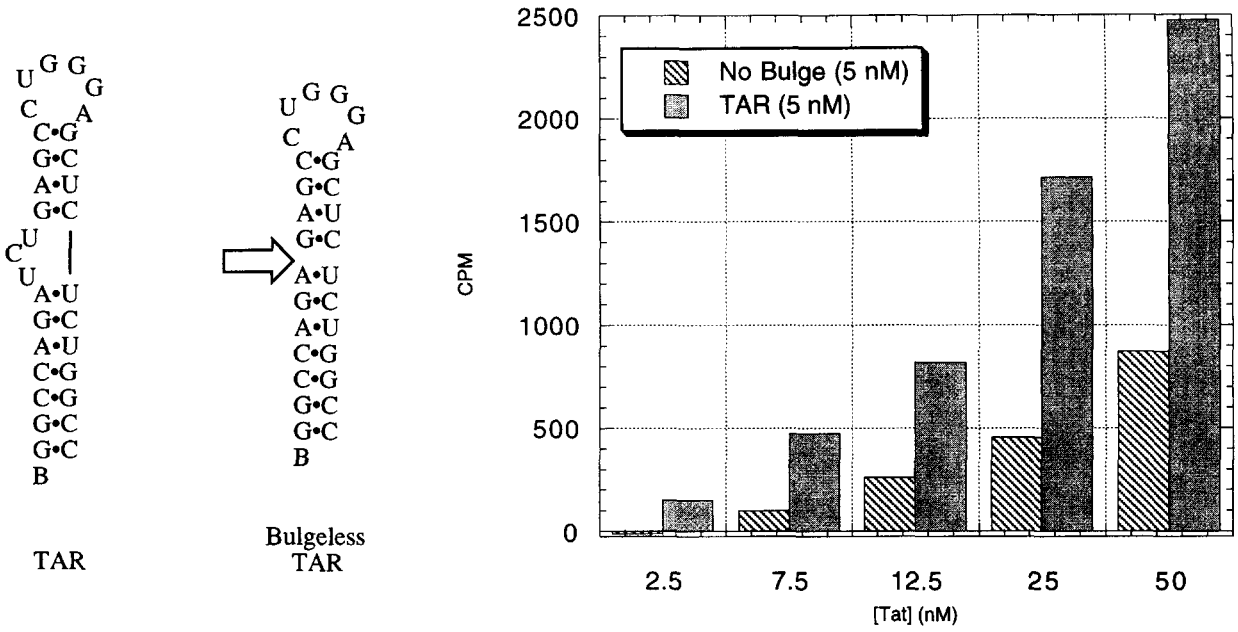

Figure 5. SPA data of Tat_{12} binding to TAR_{31} and a TAR RNA (bulgeless TAR) without the UCU bulge. Discrimination of these RNAs by Tat_{12} is clearly indicated by the data on the right. Preferential binding of Tat_{12} to wild-type TAR_{31} was found.

labeled Tat_{12} and biotinylated TAR RNA were utilized. After binding TAR RNA to the bead through the biotin–streptavidin interaction, radiolabeled Tat_{12} could be added to the reaction and the amount of light given off quantitated (Fig. 3B). It is known that small Tat peptides will discriminate between TAR RNA and mutant TAR RNA which does not contain the bulge region required for Tat binding by a factor of 20–30 in dissociation constant.[18] Performing a titration with these RNAs immobilized on a solid surface showed preferential binding of Tat with TAR RNA. As can be seen in Figure 5, the Tat_{12} peptide does indeed discriminate between the wild-type and mutant TAR RNA on the bead at all concentrations examined, confirming that the surface-bound interaction is similar to that observed in solution. Although it was not possible to determine dissociation constants for the Tat–TAR interaction using this assay,[19] it is still an effective tool for obtaining qualitative and 'yes/no' type results.

The filtration assay has also been generally used to study protein–nucleic acid interactions including the binding of the full-length Tat protein with TAR RNA.[20] In our Tat–TAR binding studies, the filter media used, nitrocellulose, was chosen empirically by testing many different membranes for their ability to retain the Tat protein and the Tat protein–TAR complex. This assay also utilizes ^{32}P-labeled TAR RNA, but instead separates free RNA from the complex by filtration through the membrane. Since the protein adheres to the membrane material, protein-bound RNA is also captured while free RNA passes through the membrane (Fig. 3C). After filtration, both the membrane and the filtrate can be counted to quantitate the amounts of free RNA and bound RNA. Dissociation constants can again be determined by titrating the RNA with varying amounts of protein (Fig. 6). Our assay yielded values of approximately 1 nM for the Tat protein–TAR RNA interaction, consistent with values found in the literature.[20] This technique is efficient, amenable to high-throughput methodologies, and can provide both quantitative and qualitative results.

ESI-MS has demonstrated capabilities for measuring molecular weights for large (>150 kDa) biomolecules and has shown utility for studying molecular interactions composed largely of noncovalent forces.[21] The analyte solution is delivered to the electrospray ionization source, which is held at a high electric field. The ESI process produces multiply charged gas phase ions from the highly charged, evaporating droplets. A distribution of charge states (multiply protonated in the case

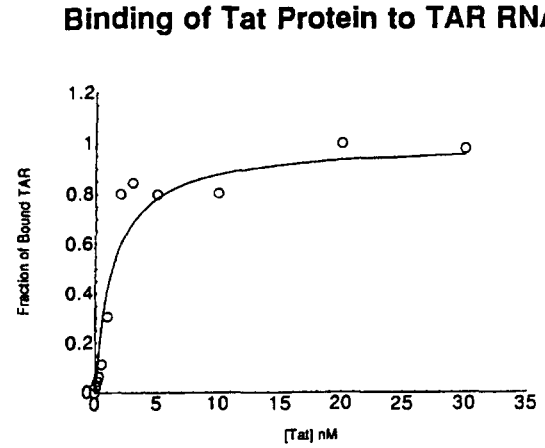

Figure 6. Filtration data of Tat protein binding to TAR_{31}. The fraction of Tat–TAR_{31} complex was determined from the radioactively labeled TAR_{31} remaining on the filter. From the titration studies, a binding constant of 1 nM was determined for Tat protein.

of positive ion ESI and multiply deprotonated for negative ion ESI) is typically observed in the ESI mass spectrum. Each multiply charged ion represents an independent measurement of the analyte's molecular weight.

ESI-MS has been applied to the study of noncovalent complexes.[21] The gentleness of the ionization process allows weakly bound, intact complexes to be detected. Several types of biomolecule interactions (e.g., protein-cofactor, protein–metal ions, quaternary structures, etc.) have been studied by ESI-MS, including DNA duplexes and protein–DNA complexes. The stoichiometry of the binding partners can be deduced easily by mass measurement of the complex. We examined the binding of the Tat peptide to TAR RNA under various conditions by ESI-MS.

For instance, negative ion ESI-MS of a solution containing Tat_{40} (M_r 4644) and TAR_{31} (M_r 9941) yields a 14.5 kDa peptide–RNA complex consistent for a 1:1 stoichiometry (Fig. 7). Increasing the Tat peptide concentration yields a 2:1 peptide–RNA complex as the maximum observed stoichiometry. To test whether the specificity of the peptide–RNA interaction is mirrored by the ESI-MS data, competitive binding experiments were performed. Mutants of TAR_{31} were studied, including a TAR_{28} RNA with the three-residue UCU bulge removed. Under competitive binding conditions where the total RNA concentration equals the protein concentration in solution, ESI mass spectra show that Tat peptide affinity for TAR RNA is greatly reduced for the bulgeless 28-mer RNA (Fig. 8); this is consistent with solution phase measurements. These results suggest that ESI mass spectra of protein–RNA complexes reflect the specific interactions found in solution.[22]

In addition to studying the Tat–TAR interaction, all of these methods can also be used to examine the effects

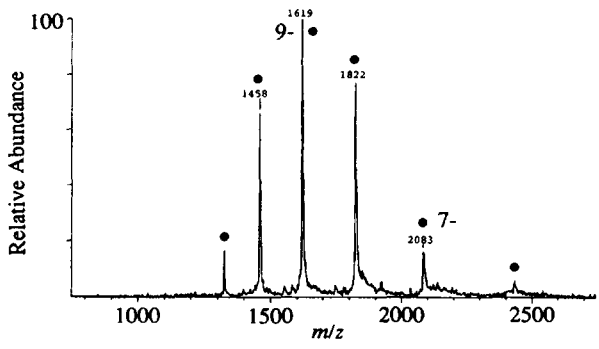

Figure 7. Negative ion ESI mass spectrum of the Tat peptide (40 residues, M_r 4644)-TAR RNA (31-mer, M_r 9941) complex. Tat peptide (26 μM) was added to a solution containing previously annealed TAR (13 μM), 0.3 mM CDTA, 10% (v/v) methanol, and 10 mM ammonium acetate, pH 6.9. The ● symbols represent peaks for the 1:1 Tat–TAR complex (M_r 14585) with various charge states. (For clarity, only the peaks for the $(M\text{-}7H)^{7-}$ ion at *m/z* 2083 and $(M\text{-}9H)^{9-}$ ion at *m/z* 1619 are indicated).

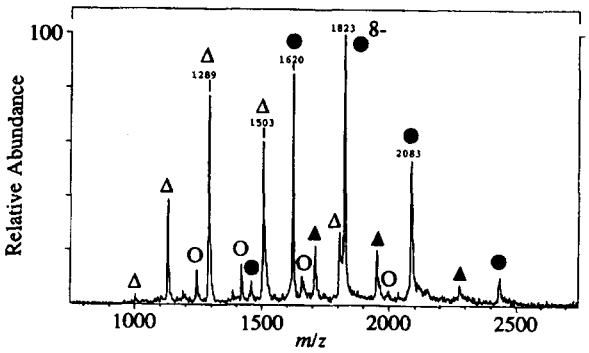

Figure 8. Negative ion electrospray ionization mass spectrum from a solution containing Tat_{40} peptide (20 μM), TAR_{31} RNA (10 μM), and TAR_{28} RNA (10 μM) (no bulge, M_r 9023) in 10 mM ammonium acetate, pH 6.9 with 0.3 mM CDTA and 10% (v/v) methanol. The following symbols represent the peaks for the various multiply charged ions: ○ = free TAR_{31}, Δ = free TAR_{28}, ● = Tat_{40} – TAR_{31} 1:1 complex (M_r 14585), ▲ = Tat_{40} – TAR_{28} 1:1 complex (M_r 13667). Formation of the 1:1 Tat_{40} – TAR_{31} complex was much more preferable than that of Tat_{40} – TAR_{28}.

of potential inhibitors. In each of these methods, relative amounts of the free Tat or TAR and Tat–TAR complex can be readily determined. Inhibitors for the Tat–TAR interaction will be identified based on a decreased amount of Tat–TAR complex than that of the control sample which contains only the Tat and TAR. As an example, we have applied these methods to study Tat–TAR inhibition with a group of RNA-binding ligands—aminoglycoside antibiotics.[23] Inhibition of Tat–TAR interaction by aminoglycoside antibiotics will be discussed in the following section.

Furthermore, due to the nature of these methods, it is not always possible to discriminate whether an inhibitor exerts its effect by binding to Tat or TAR. To fully explore the structure–activity relationship (SAR) of a series of inhibitors, however, the molecular target of these inhibitors must first be identified. Of all the methods discussed above, only ESI-MS can readily distinguish inhibitors that bind to Tat, TAR, or the Tat–TAR complex by directly measuring the appropriate molecular weight. The fact that ESI-MS experiments on the Tat–TAR interaction are consistent with those obtained from solution studies encouraged us to further investigate its application in this regard. Using aminoglycoside antibiotics as examples, the use of ESI-MS in distinguishing small molecules that interact with TAR RNA will also be discussed in the following section.

Small-molecule intervention of Tat–TAR interaction

Aminoglycoside antibiotics represent one of the first examples of small molecules that inhibit HIV-1 Tat–TAR interaction. We have previously reported that aminoglycoside antibiotics inhibit Tat–TAR interaction by binding directly to TAR RNA.[7] Table 1 summarizes the inhibition and direct-binding results of three aminoglycosides; neomycin, streptomycin, and gentamicin. These aminoglycosides inhibit the binding of

Table 1. Aminoglycoside antibiotics binding and inhibition data

Aminoglycosides	IC_{50} (μM)	C_{50} (μM)
Neomycin	0.92 ± 0.09	0.7 ± 0.2
Streptomycin	9.5 ± 0.8	2.4 ± 0.2
Gentamicin	45 ± 4	4.3 ± 0.9

Tat_{40} to TAR_{31} with IC_{50} values of 0.92, 9.5, and 45 μM for neomycin, streptomycin, and gentamicin, respectively. Inhibition of Tat_{12} peptide binding to TAR_{31} by aminoglycosides was also evident using the SPA (data not shown). The gel mobility shift assay showed neomycin to be a better inhibitor of Tat_{12}–TAR_{31} interaction than streptomycin, and filtration assay data also indicate that neomycin inhibited the interaction of the full-length Tat protein with the TAR_{31} (data not shown). All of the three methods discussed in Figure 2—gel mobility shift, SPA, and filtration methods—generated similar results when used to examine inhibitory effects of aminoglycoside antibiotics against the Tat–TAR interaction.

We have also demonstrated that these antibiotics disrupt the Tat–TAR interaction by binding to TAR RNA and not to Tat (peptide or protein). In the absence of Tat_{40} peptide, neomycin, streptomycin, and gentamicin were found to interact with TAR_{31} and induce mobility shifts in TAR_{31} on a native polyacrylamide gel. As shown in Figure 9, neomycin forms complexes with TAR in a concentration-dependent manner. Formation of antibiotic–TAR_{31} complexes as a function of drug concentration was used to determine the binding affinity for each aminoglycoside. By defining a measurement of binding affinity, C_{50} (a concentration at which 50% of the total RNA is bound by antibiotic based on a gel mobility shift experiment), the antibiotics complexed to TAR_{31} in the following order: neomycin > streptomycin > gentamicin (Table 1). The aminoglycoside–TAR binding results and the Tat_{40} inhibition data indicate that the better RNA binders (e.g., neomycin) demonstrate larger inhibition effects (smaller IC_{50} values) on Tat_{40} binding to TAR_{31}. Simple inspection verifies that the IC_{50} or C_{50} values are not a simple function of the number of positive charges contained in these small molecules.

The binding of neomycin to TAR RNA can be further demonstrated by ESI-MS. Gas-phase molecules with mass-to-charge values (m/z) corresponding to neomycin–TAR RNA complexes were observed using ESI-MS. In these experiments, a solution of TAR RNA was titrated with increasing amounts of neomycin. In addition to free TAR RNA, complexes of neomycin–TAR at various ratios were observed. Figure 10 shows the formation of neomycin–TAR_{31} complexes as a function of drug concentration. The higher-order complexes occur at higher antibiotic concentrations and subsequent to the formation of an initial drug–TAR_{31} complex. This gas-phase observation correlates, at least qualitatively, with the results obtained from the gel mobility shift assay (Figure 9).

Competition studies in which both neomycin and streptomycin are allowed to react with TAR were also performed (Fig. 11). Both the positive- and negative-ion modes show that neomycin binds more preferentially to TAR. This is also consistent with the gel shift assay indicating that neomycin binds ≈3 times (Table 1)

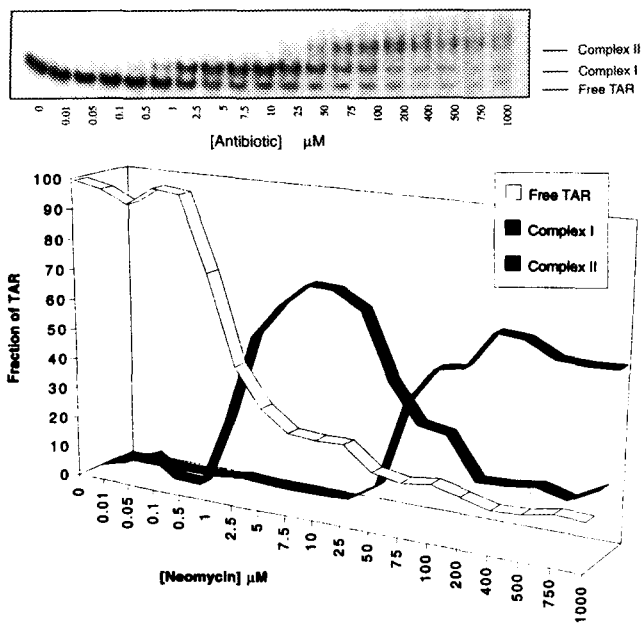

Figure 9. Direct binding of neomycin to TAR_{31}. Free TAR_{31} was titrated with increasing amount of neomycin (0–1000 μM). Top: On a nondenaturing polyacrylamide gel, free TAR_{31} and TAR_{31}–neomycin complexes were well resolved. Based on the difference in electrophoretic mobility, more than one TAR_{31}-neomycin complexes were observed. Bottom: The relative amounts of free TAR_{31}, TAR_{31}–neomycin complexes were quantitated and plotted against [neomycin] in μM.

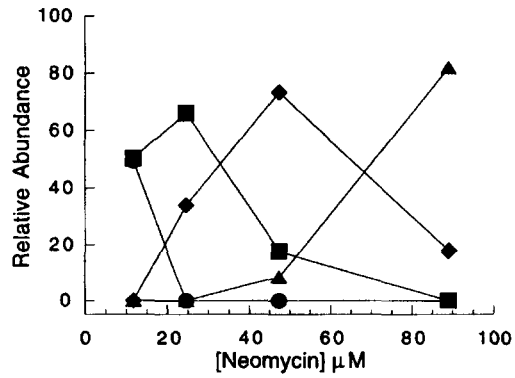

Figure 10. Direct binding of neomycin to TAR_{31} followed by negative ion ESI-MS. Free TAR_{31} (10 μM, previously annealed) was titrated with increasing amounts of neomycin (0–100 μM) in 10 mM ammonium acetate, pH 6.9 with 0.3 mM CDTA and 10% (v/v) methanol. The relative amounts of free TAR_{31} (●), TAR_{31}–neomycin 1:1 complex (■), TAR_{31}–neomycin 1:2 complex (◆), and TAR_{31}–neomycin 1:3 complex (▲) were measured by ESI-MS and plotted against [neomycin] in μM. The ESI-MS data is qualitatively consistent with the data obtained from the gel mobility shift method (see Fig. 9).

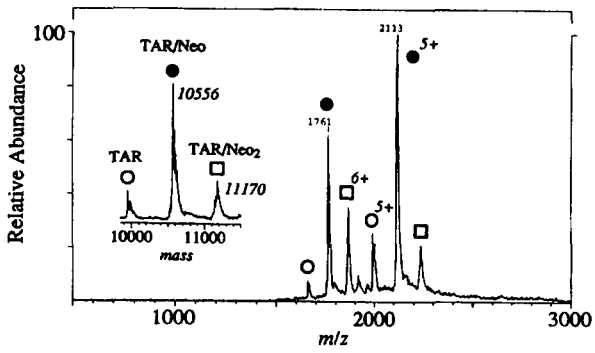

Figure 11. Competition studies of TAR_{31} with neomycin and streptomycin using positive ion ESI-MS. Equivalent amounts of neomycin (10 μM) and streptomycin (10 μM) were added to a previously annealed solution of TAR_{31} (10 μM) in 10 mM ammonium acetate, pH 6.9 with 0.3 mM CDTA, and 10% (v/v) methanol. Under these competitive binding conditions, only complexes between neomycin and TAR_{31} are observed; no complexes between streptomycin and TAR_{31} are observed.

more strongly to TAR than streptomycin. Similarly, competition studies with the Tat–TAR complex show that neomycin binds with higher affinity to the complex than streptomycin. Thus, competition studies using ESI-MS can be used to determine relative drug-binding affinities.

High-throughput screening small-molecule inhibitors of Tat–TAR interaction

The ultimate goal of our drug discovery project is to identify small molecules that inhibit Tat–TAR interactions, and therefore the life cycle of HIV-1 in infected host cells. Based on this premise and the consideration of assay throughput, a mechanism-based drug discovery program, outlined in Figure 12, was designed.

To investigate a corporate library of ≈150,000 compounds within a reasonable time frame, the primary screens should be operated with sufficient throughput. The first step in our screening strategy involved in vitro screening assays targeting HIV-1 Tat–TAR interactions. Second, inhibitors identified from the primary screens were submitted to a more laborious cell-based Tat-transactivation assay. Third, the activity of an inhibitor in blocking Tat-activated gene expression in a cellular environment was verified. And finally, compounds active in inhibiting both Tat–TAR interactions and Tat-activated transcription were submitted to HIV-1 viral infection assays to test their anti-viral activities.

Both SPA and filtration assays function as high-throughput screening methods for Tat–TAR inhibitors. Performing the SPA using the Tat_{12} peptide and TAR_{31} RNA in parallel with the filtration assay using the full-length Tat protein and TAR_{31} RNA offers us a better opportunity to identify inhibitors regardless of the assay conditions. Since the nature of these assays is different, the same sample may behave differently in each assay.

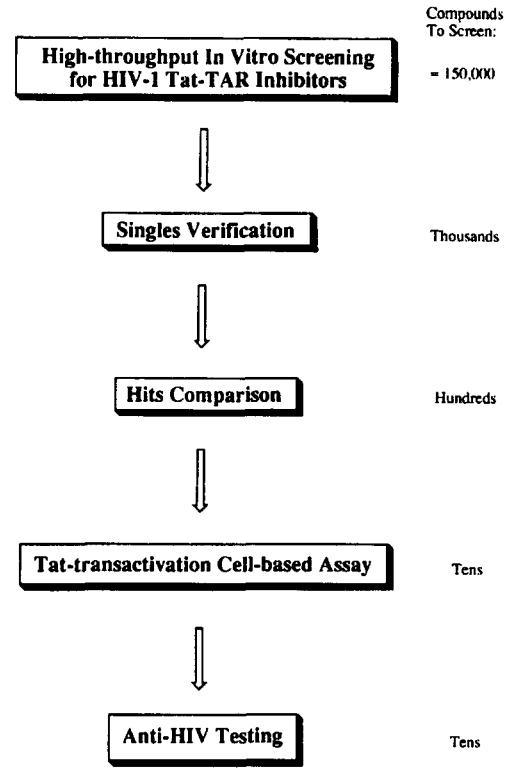

Figure 12. A drug discovery strategy for identifying anti-HIV-1 agents capable of inhibiting Tat–TAR interaction.

It is conceivable to find samples either active in both assays or active in only one assay. In addition, the use of Tat_{12} peptide in SPA, and Tat protein in the filtration assay could potentially discriminate samples that interact with Tat or TAR. For example, samples active in one (filtration) but not the other (SPA) might well interact with Tat since the same TAR_{31} was used in both assays. On the other hand, samples active in both assays might inhibit Tat–TAR interactions involving either Tat or TAR binding.

High-throughput screenings were conducted using 96-well microtiter plates. All liquid samplings were performed using a robotic workstation with minimal manual operation. Excluding the wells (columns 1 and 12) reserved for control samples, each plate simultaneously allowed the screening of 80 different samples. In four months, the entire corporate library (≈150,000 compounds) screening was completed using either the SPA or the filtration assay. Samples were tested in mixture format with each component at 20 μM concentration. A 50% or greater inhibition, compared with the controls, defined a positive result. Control samples contained no potential inhibitors. A proprietary method was used to deconvolute single, active components from the mixtures.

From the entire library, about 3200 active compounds were found in the SPA screen while about 2000 compounds showed ≥50% inhibitory effect in the filtration assay. This represents a 1–2% success rate in

identifying active compounds with these high-throughput assays. The results of a typical sample plate obtained from the filtration assay are shown in Figure 13.

Since primary screens investigated mixtures of dissolved compounds, it was necessary to verify these results using freshly prepared compounds in singular form. In this verification process, each active compound was acquired in solid form, dissolved in DMSO, and investigated at four different concentrations. Using either a gel mobility shift assay with Tat_{40} and TAR_{31} or a filtration assay, similar to that used in the high-throughput screening, we re-examined thousands of primary hits. About one-third of these singletons (hundreds) showed dose-dependent activities (IC_{50} values $\leq$ 50 μM) in this verification process.

As mentioned earlier, a comparison of active compounds identified from the two primary assays should assist in classifying the inhibitors for Tat–TAR interaction. Interestingly, the hits that were active in both assays represent only about 12% of the combined hits. About another 20% of the combined hits represent similar but not identical hits in both assays. The rest of the 68% represents compounds displayed in one but not the other assay. From this comparison of hits, classifications of hits were made. This process allowed us to select representatives from each class and to establish priority of the Tat–TAR inhibitors for follow-up studies in the cellular assays.

To investigate the cellular activities of the Tat–TAR inhibitors, a Tat-transactivation assay was established.[10] As illustrated in Figure 14, this assay is performed in a HeLa cell line constitutively expressing Tat. The expression of Tat in the HeLa cells is regulated by a promoter derived from Rouse sarcoma virus (RSV) and a consistent level of endogenous Tat can be determined by immunoblotting. The Tat-expressing HeLa cells are then transiently transfected by a plasmid (pHIV*lacZ*) containing a promoter domain derived from HIV-1 3′-LTR and a *lacZ* reporter gene. The HIV-1 LTR promoter containing TAR RNA element can be bound and activated by the Tat protein. The expression of the *lacZ* gene is controlled by the LTR promoter and the products of the expression are β-galactosidases. The amount of expressed β-galactosidase (determined by the enzymatic activity in hydrolyzing a chromogenic substrate) serves as an indicator for Tat–TAR interaction in the absence or presence of added inhibitors. For each Tat–TAR inhibitor, 50% inhibitory concentration (IC_{50}) can be determined.

A similar assay using the cytomegalovirus (CMV) promoter-driven reporter genes[24] was constructed to identify compounds exerting their functions specifically at the Tat–TAR interaction. This assay utilizes a similar Tat-expressing HeLa cell line as described in Figure 14. However, the HeLa cells in this assay are transiently transfected with a plasmid (pCMV*lacZ*) containing a CMV promoter and a *lacZ* gene. The CMV promoter does not include a TAR element and its activation is Tat-independent. Therefore, the expression of the *lacZ*

	1	2	3	4	5	6	7	8	9	10	11	12
A	16488	16614	17304	16553	15540	15453	15160	746	15887	16968	15974	356
B	16054	4470	17605	17294	16001	14062	16091	15079	16544	16087	16434	347
C	16592	16775	17096	16399	15792	14884	15634	15397	16584	16834	17067	350
D	16486	16187	15086	17311	14198	16230	16096	1073	16029	16199	16525	348
E	16164	16311	14173	16766	15317	11533	14378	5335	15227	15580	15341	350
F	15757	17009	15870	16844	15869	15529	16080	15473	15878	12734	15751	337
G	16103	16621	15855	16582	16207	16391	16459	980	16103	15455	15894	338
H	15529	16615	13575	14885	16204	15892	15882	14149	15796	15886	15815	388

	1	2	3	4	5	6	7	8	9	10	11	12
A		−3	−7	−3	4	4	6		2	−5	2	
B			−9	−7	1	13	0	7	−3	0	−2	
C		−4	−6	−2	2	8	3	5	−3	−4	−6	
D		0	7	−7	12	−1	0		1	0	−2	
E		−1	12	−4	5	29	11		6	4	5	
F		−5	2	−4	2	4	0	4	2	22	3	
G		−3	2	−3	0	−2	−2		0	4	2	
H		−3	16	8	0	2	2	13	2	2	2	

Figure 13. A typical example of high-throughput screening data obtained from Tat protein-TAR_{31} filtration assay. TAR_{31} is radioactively labeled at the 3′-end with ^{32}P-pCp. Top: Raw data of a 96-well microtiter plate. Column 1 represents data (eight repeats) of Tat protein–TAR_{31} interaction in the absence of any potential inhibitors. Column 12 represents data of samples containing TAR_{31} only. Wells in columns 2–10 contain Tat–TAR complexes in the presence of potential inhibitors. Bottom: Percentage of inhibition was obtained for samples in each well (columns 2–10). Active samples such as those in wells A8, B2, D8, E8, and G8 can be readily identified (shaded wells).

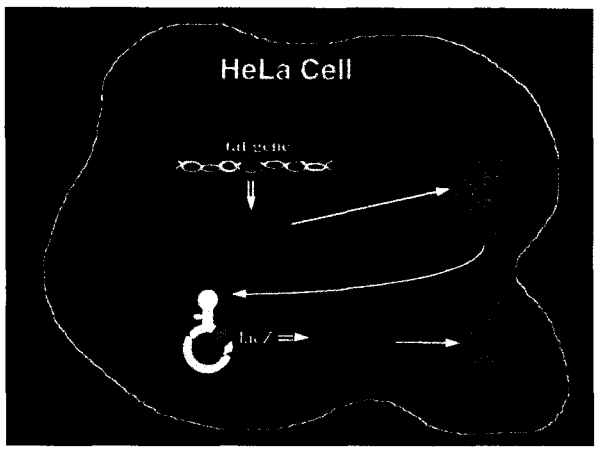

Figure 14. A schematic representation of the HeLa cell line used in the Tat-transactivation assay. In this cell line, Tat is constitutely expressed. The expression of *lacZ* reporter gene is under the control of HIV-1 LTR promoter which contains TAR RNA.

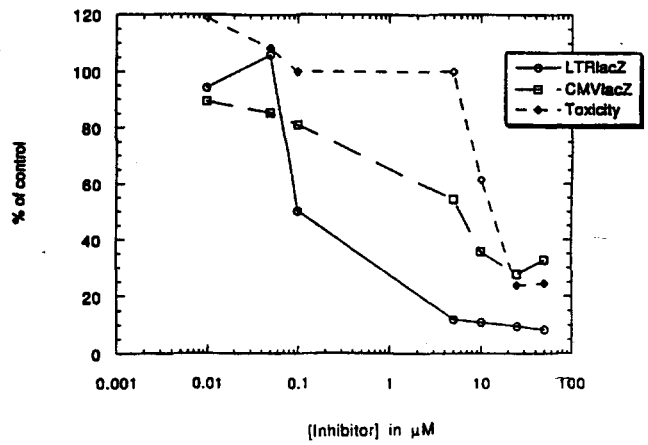

Figure 15. Inhibition data obtained for a Tat–TAR inhibitor. A dose-dependent inhibition was found for this Tat–TAR inhibitor in the HeLa cells transfected with pHIV*lacZ*. The IC_{50} value is 0.2 μM. This compound was also found to be relatively nontoxic (TI_{50} value of ≈20 μM) and selective (IC_{50} value of ≈10 μM in cells transfected with pCMV*lacZ*) at the effective drug concentration.

in these cells should be irrelevant to Tat–TAR interaction. Compounds active in cells transfected with pHIV*lacZ* but not in those transfected with pCMV*lacZ* are considered selective. If the inhibition is found in both cell lines, the inhibition may involve a mechanism other than Tat–TAR interaction. Therefore, the results obtained from both cell lines are useful in determining the activity and selectivity of the Tat–TAR inhibitors. Furthermore, the cytotoxicity of the tested compounds in HeLa cells can also be investigated. The concentration required to cause 50% cell death (TC_{50}) can be determined for each drug. Regardless of their inhibitory effects, compounds cytotoxic to HeLa cells are normally given low priority for further studies.

Approximately 500 Tat–TAR inhibitors were investigated in this Tat-transactivation assay; these compounds were originally identified as Tat–TAR inhibitors from primary assays. Among them, approximately 50 compounds exhibited dose-dependent cellular activities (IC_{50} values ≤ 50 μM). Out of these active compounds, approximately 20 compounds are relatively nontoxic (therapeutic index, TC_{50}/IC_{50}, ≥ 5) and considered selective for Tat-dependent transcription (IC_{50} obtained from HeLa cells transfected with pHIV*lacZ* at least fivefold greater than that from cells transfected with pCMV*lacZ*).

As an example, the cellular data of a Tat–TAR inhibitor are shown in Figure 15. This inhibitor exhibits dose-dependent activity against the expression of the *lacZ* gene with an IC_{50} value of 0.2 μM. The TC_{50} (drug concentration that causes 50% of the cells to die) value of this compound was found to be 20 μM. The therapeutic index of this compound is therefore around 100. At similar concentrations, this compound was relatively ineffective in blocking *lacZ* gene expression activated by the CMV promoter (IC_{50} of this compound is ≈10 μM.) These results indicate that this Tat–TAR inhibitor selectively intervenes the Tat-activated transcriptional process in the HeLa cells with a reasonable therapeutic index.

In comparison, two previously reported Tat-inhibitors, a benzodiazepine analogue (Ro 5-3335)[8a] and camptothecin,[25] were also examined in our Tat-transactivation assays. These two compounds, originally identified from cellular assays similar to the one described above, were active in inhibiting Tat-activated gene expression and in blocking HIV-1 infection. However, the mechanism of action of these compounds is not fully understood. A comparison of these compounds and our Tat–TAR inhibitor in Tat–TAR inhibition assays and Tat-transactivation cellular assays is presented in Table 2. The cellular assays yielded similar IC_{50} values (0.2–3 μM) for all three compounds. They all had reasonable

Table 2. Inhibitory activity of three compounds in Tat–TAR interaction and Tat-transactivation cellular assays

	Tat/TAR inhibition		Tat-transactivation cell-based assay			
	Tat_{40} peptide IC_{50} (μM)	Tat protein IC_{50} (μM)	HIV LTR-driven β-gal expression IC_{50} (μM)	CMV IE-driven β-gal expression IC_{50} (μM)	Cytotoxicity TC_{50} (μM)	Therapeutic index TC_{50}/IC_{50}
Tat/TAR inhibitor	0.3	0.4	0.2	10	20	100
Ro 5-3335 (benzodiazepine)	Not active	Not active	3	>100	>100	>33
Camptothecin	Not active	Not active	0.7	10	20	30

selectivity for HIV-1 LTR-activated *lacZ* expression, and high therapeutic indices against HeLa cells. Unlike our Tat–TAR inhibitor, the Ro 5-3335 and camptothecin were not active in our Tat–TAR inhibition studies. A mechanism other than Tat–TAR inhibition must be responsible for their cellular activities in HIV-1 regulation.

Increasing numbers of biological functions have been found for Tat.[26] Unless the biological targets and their modes of action are well defined, it is usually difficult to explore a satisfactory SAR or pharmacological properties of any inhibitors (such as Ro 5-3335) identified from cellular assays. Our approach to initially select small-molecule inhibitors that act on HIV-1 Tat–TAR interaction and to verify their activities in a cellular environment is unique from others. The well-studied Tat–TAR model provides a basis for SAR studies around some identified inhibitors. These SAR data can then be verified or modified using biological data obtained from cellular assays. The fact that at least one of our inhibitors is active in blocking both the Tat–TAR interaction and Tat-activated gene expression in whole cell assays provides a reasonable working model for further SAR and anti-viral studies.

Small-molecule inhibitors identified from both Tat–TAR and Tat-transactivation screens represent high-value leads for further anti-HIV-1 studies. These inhibitors are currently under investigation using several HIV-1 infection assays including both acute and chronic infection models. For compounds active in anti-viral assays, their mode of action can be verified using RNA transcript analysis. Since the Tat–TAR interaction correlates with Tat-activated transcription, the amount of full-length transcript of HIV-1 mRNA in the infected cells serves as a good marker for Tat–TAR inhibition.

Summary

Tat–TAR interaction, crucial for HIV-1 viral replication, represents a potential therapeutic target for AIDS treatment. This aspect has been verified in cellular infection assays, using macromolecular agents including analogues of Tat or TAR. Small-molecule drugs inhibiting HIV-1 infection by an intervening Tat–TAR interaction could supplement the existing therapeutics targeting other molecular entities such as reverse transcriptase or protease.

We designed a drug-discovery program focusing on HIV-1 Tat protein–TAR RNA inhibition. This Tat–TAR interaction-based approach begins with high-throughput screening for small-molecule inhibitors. Methods employed to study HIV-1 Tat–TAR interaction include gel mobility shift, SPA, filtration, and electrospray ionization mass spectrometry. Based on these methods, the creation of in vitro high-throughput screening assays rapidly identified Tat–TAR inhibitors from our corporate compound library. Tat-activated reporter gene assays investigated the cellular activities of these inhibitors. Evaluating Tat–TAR inhibitors on their cellular activity, selectivity, and toxicity led to selection for further testing in anti-HIV-1 infection assays. The anti-viral activity and the cellular mechanism of certain Tat–TAR inhibitors are currently under investigation.

Experimental

Material

Camptothecin and all aminoglycoside antibiotics were obtained from Sigma and used without further purification. Ro 5-3335 was a generous gift from Hoffman-La Roche, Nutley, NJ.

Preparation and characterization of Tat and TAR

Both of the Tat peptides used in this study (12 and 40 amino acids in length) were prepared chemically using standard solid phase methodology utilizing Boc-protected amino acids.[27] The peptides were deprotected using HF, purified by reverse-phase HPLC, and characterized by ESI-MS. Tat protein was overexpressed in *E. coli* according to literature reports.[28] The recombinant Tat was identified by SDS gel electrophoresis with a mobility similar to that of a molecular marker with $\approx$15,000 daltons. The fractions containing Tat were pooled, treated with dithiothreitol in guanidine hydrochloride, and purified by HPLC. The purified Tat was characterized by amino acid sequencing (from N-terminus to residue 55) and ESI-MS. The transactivation activity of the purified rTat was further verified by scrape-loading the protein into a reporter cell line (HIV-LTR*lacZ* HeLa). TAR_{31} used in all studies was produced by solid phase methodologies utilizing 5′-DMT, 2′-TBDMS protected phosphoramidites of the ribonucleotides.[29] Typically coupling yields of between 98 and 99% per step were obtained. After base treatment in 3:1 NH_4OH/EtOH at 55 °C to deprotect and cleave the RNA from the solid support, the TBDMS groups were removed with TBAF in THF. After desalting, the RNA was purified by PAGE and removed from the gel slice by the crush and soak method. Typical overall yields after purification were approximately 10% (1 μmol scale synthesis). For ESI-MS experiments, RNA samples were further desalted by cold ethanol precipitation. RNA concentrations were determined by UV, the RNA aliquoted into small samples, lyophilized, and stored dry at −20 °C. Biotin was added to the 5′-end of the TAR RNA during synthesis using the BioTEG phosphoramidites (Glen Research) and purified as above. When appropriate, RNA was labeled at the 3′-end using 3′,5′-[5′-^{32}P]-cytidinebisphosphate and T4 RNA ligase.

Mass spectrometry

ESI-MS was performed with a double focusing hybrid mass spectrometer (Finnigan MAT 900Q, Bremen, Germany) with a mass-to-charge (m/z) range of 10,000

at 5 kV full acceleration potential. A position-and-time-resolved-ion-counting (PATRIC) scanning focal plane detector was used. Peptide and RNA solutions were buffered with 10–25 mM ammonium acetate, pH 6.9. For the peptide–RNA experiments, methanol to the 10% (v/v) level was added to the aqueous ammonium acetate ESI-MS solution. This enhanced the stability of ESI-MS signal without altering the resulting spectra to a significant extent for these systems. Solution flow rates delivered to the ESI source were typically in the 0.5–1.0 μL min^{-1} range.

High-throughput screening

A high-throughput filtration assay capable of screening compounds that inhibit HIV-1 Tat protein binding to TAR RNA has been established. The assay utilizes 96-well filter plates (Multiscreen-HA Filtration Plates, Millipore) with nitrocellulose membrane incorporated at the bottom of each well. All liquid samplings were performed using a robot workstation (Biomek 1000, Beckman). In each well the filter is pre-wetted with cold buffer solution and then a solution (96 μL) of 3′-^{32}P-labeled TAR_{31} is added, followed by addition of 4 μL of the compound mixture (in DMSO). After standing about 10 min for equilibration, 100 μL of Tat protein solution is added. All solutions contain 10 mM Tris-HCl, pH 7.5, 50 mM NaCl, 5 mM $MgCl_2$, 5% glycerol, 0.01% Nonidet-P40, 10 mM dithiothreitol. After mixing and equilibration for about 10 min, the solutions in each well are simultaneously filtered using Multiscreen Vacuum Manifold (Millipore). The filters are washed with cold buffer once before determining their radioactivities using Microbeta Liquid Scintillation Counter (Model 1450, Wallac). The relative amounts of free and bound-TAR can be determined by quantitation of the radioactivity on each filter.

A high-throughput scintillation proximity assay was established using ^{125}I-Tat_{12} and biotinylated TAR_{31} RNA. All solutions were prepared using a buffer consisting of 10 mM Tris–HCl, pH 7.4, 70 mM NaCl, 0.1 mM EDTA, 0.01% Nonidet-P40. All liquid handling was performed using a Biomek 1000 workstation. To 2 mL of buffer was added 400 μL of streptavidin-coated SPA beads (Amersham, 10 μg/μL) followed by 500 μL of 100 nM 5′-biotin TAR RNA. The solution was vortexed and another 4.1 mL of buffer solution was added. The solution was then dispensed into a 96-well microtiter plate (70 μL/well). Five microliters of DMSO or 1 mM sample in DMSO was then added and the solution mixed by drawing into and out of a pipet three to four times (70 μL volume). A 25 μL quantity of ^{125}I-Tat_{12} (250 nM, prepared from 25 μL of 10 μM unlabeled peptide, 200 μL of 50 nM labeled peptide, and 775 μL of buffer) was then added to each well. Tat_{12} was radioiodinated on tyrosine residue with ^{125}I using the chloramine-T method and isolated by reverse phase HPLC. The plate was then sealed, inverted five to six times and allowed to stand for ≈20 min before counting on a Microbeta Counter.

Tat-transactivation cell-based assays

HeLa cells (American Type Culture Collection) maintained in Dulbecco's modified Eagle's medium (DMEM, Life Technologies), were supplemented with 10% fetal calf serum (BioWhittaker). pRSVtat, a vector in which Tat expression was driven by the RSV promoter, was a gift from B. M. Peterlin (University of California, San Francisco) and used to stably transfect HeLa cells. The resulting cell line expresses constitutively Tat proteins. In this cell line, further transfection was performed with a pHIV*lacZ* vector (NIH AIDS Research and Reference Reagent Program), a construct in which *lacZ* gene expression is driven by HIV-1 3′-LTR domain. A collection of HeLa pRSVtat cells (4×10^6 cells/mL) was electroporated with 5 μg of pHIV*lacZ* using a Gene Pulser (Bio-Rad) at 230 volts and 960 μF. For inhibition studies, compounds were dissolved in DMSO and diluted with DMEM supplemented with 10% fetal calf serum. HeLa cells (2×10^4 cells/100 mL DMEM) were incubated with various amounts of inhibitors in 96-well microtiter plates. Under similar conditions, cell viability in the presence of added compounds were also determined.

The sample plates were incubated for 48 h in a 5% CO_2 incubator (temperature controlled at 37 °C). The cells were then washed twice with PBS. One hundred microliters of reporter lysis buffer (Promega) were then added to each well. The cells were lysed for 15 min and 100 μL assay buffer (80 mM sodium phosphate buffer, pH 7.4, 102 mM 2-mercaptoethanol, 9 mM $MgCl_2$, and 8 mM chlorophenol red-β-D-galactopyranoside) were added to determine the amount of β-galactosidase in the lysates. The plates were incubated at 37 °C for 30 min and absorbance was read at 570 nm on a ThermoMax microplate reader (Molecular Devices). Cell viability was determined by adding 0.3 mM XTT (2,3-bis(2-methoxy-4-nitro-5-sulfophenyl)-2H-tetrazonium-5-carboxanilide salt) (Sigma) to the cells. After 2 h incubation, 25 μL of lysis buffer containing 0.5% Nonidet-P40 and 0.1 % SDS in PBS buffer, pH 7.4, was added to each well and absorbance between 450–650 nM was obtained to calculate IC_{50} and TC_{50} values.

References

1. (a) Vaishnav, Y. N.; Wong-Staal, F. *Annu. Rev. Biochem.* **1991**, *60*, 577. (b) Karn, J.; Graeble, M. A. *Trends in Genet.* **1992**, *8*, 365. (c) Fisher, A. G.; Feinberg, M. B.; Josephs, S. F.; Harper, M. E.; Marselle, L. M.; Reyes, G.; Gonda, M. A., Aldovini, A.; Debouk, C.; Gallo, R. C.; Wong-Staal, F. *Nature (London)* **1986**, *320*, 367.

2. (a) Muesing, M. A.; Smith, D. H; Capon, D. J. *Cell* **1987**, *48*, 691. (b) Feng, S.; Holland, E. C. *Nature (London)* **1988**, *334*, 165. (c) Berkhout, B.; Silverman, R.; Jeang, K.-T. *Cell* **1989**, *59*, 273.

3. (a) Roy, S.; Delling, U.; Chen, C.-H.; Rosen, C. A.; Sonenberg, N. *Genes Develop.* **1990**, *4*, 1365. (b) Dingwall, C.; Ernberg, I.; Gait, M. J.; Green, S. M.; Heaphy, S.; Karn, J.; Lowe, A. D.; Singh, M.; Skinner, M. A. *EMBO J.* **1990**, *9*, 4145. (c) Delling, U.; Reid, L. S.; Barnett, R. W.; Ma, M. Y.-X.;

Climie, S.; Sumner-Smith, M.; Sonenberg, N. *J. Virol.* **1992**, *65*, 7012.

4. Johnston, M. I.; Hoth, D. F. *Science* **1993**, *260*, 1286.

5. (a) Chodakewitz, J. A.; Emini, E. A. PCT Int. Appl. CODEN: PIXXD2. WO 9623509 A1 960808. (b) Larder, B. A.; Kohli, A.; Bloor, S.; Kemp, S. D., Harrigan, P. R.; Schooley, R. T.; Lange, J. M. A.; Pennington, K. N.; St Clair, M. H. *J. Virol.* **1996**, *70*, 5922. (c) Katlama, C.; Ingrand, D.; Loveday, C.; Clumeck, N.; Mallolas, J.; Staszewski, S.; Johnson, M.; Hill, A. M. *J. Am. Med. Assoc.* **1996**, *276*, 118.

6. (a) Sullenger, B. A.; Gallardo, H. F.; Ungers, G. E.; Gilboa, E. *J. Virol.* **1991**, *65*, 6811. (b) Ecker, D. J.; Vickers, T. A.; Bruice, T. W.; Freier, S. M.; Jenison, R. D.; Manoharan, M.; Zounes, M. *Science* **1992**, *257*, 958. (c) HIV Tat Inhibitor from Allelix Enters Phase I Trials. *Antiviral Agents Bulletin* **1993**, *6*, 291

7. Mei, H.-Y.; Galan, A. A.; Halim, N. S.; Mack, D. P.; Moreland, D. W.; Sanders, K. B.; Truong, H. N.; Czarnik, A. W. *Bioorg. Med. Chem. Lett.* **1995**, *5*, 2755.

8. (a) Hsu, M.-C.; Schutt, A. D.; Holly, M.; Slice, L. W.; Sherman, M. I.; Richman, D. D.; Potash, M. J.; Volsky, D. J. *Science* **1991**, *254*, 1799. (b) Michne, W. F.; Schroeder, J. D.; Bailey, T. R. *J. Med. Chem.* **1993**, *36*, 2701.

9. Hsu, M.-C.; Cupelli, L. A. *J. Virol.* **1995**, *69*, 2640.

10. Young, D. C.; Kingsley, S. D.; Ryan, K. A.; Dutko, F. J. *Anal. Biochem.* **1993**, *215*, 24.

11. Sharp, P. A.; Marciniak, R. A. *Cell* **1989**, *59*, 229.

12. Tao, J.; Frankel, A. D. *Proc. Natl. Acad. Sci. U.S.A.* **1992**, *89*, 2723.

13. (a) Hauber, J.; Malim, M. I. I.; Cullen, B. R. *J. Virol.* **1989**, *63*, 1181. (b) Calnan, B. J.; Tidor, B.; Biancalana, S.; Hudson, D.; Frankel, A. D. *Science* **1991**, *252*, 1167.

14. (a) Weeks, K. M.; Ampe, C.; Schultz, S. C.; Steitz, T. A.; Crothers, D. M. *Science* **1990**, *249*, 1281. (b) Frankel, A. D. *Protein Science* **1992**, *1*, 1539.

15. (a) Puglisi, J. D.; Tan, R.; Calnan, B. J.; Frankel, A. D.; Williamson, J. R. *Science* **1992**, *257*, 76. (b) Aboul-ela, F.; Karn, J.; Varani, G. *J. Mol. Biol.* **1995**, *253*, 313. (c) Aboul-ela, F.; Karn, J.; Varani, G. *Nucleic Acids Res.* **1996**, *24*, 3974.

16. Long, K. S.; Crothers, D. M. *Biochemistry* **1995**, *34*, 8885.

17. Uderfriend, S.; Gerber, L.; Nelson, N. *Anal. Biochem.* **1987**, *161*, 494.

18. (a) Weeks, K. M.; Crothers, D. M. *Biochem*, **1992**, *31*, 10281. (b) Calnan, B. J.; Biancalana, S.; Hudson, D.; Frankel, A. D. *Genes Dev.* **1991**, *5*, 201.

19. A dissociation constant was not determined due to the fact that the titration data did not show binding saturation at the concentrations studied. Since the concentrations examined should have been sufficient to reach saturation, this may indicate a difference between SPA and other techniques for observing the Tat–TAR interaction. A number of possibilities exist to explain this difference including that in the SPA technique the RNA is bound to a solid-phase particle and that the assay was optimized for signal-to-noise ratio. Either of these explanations would affect apparent values for the dissociation constant. Further work will be needed to understand the thermodynamic and kinetic aspects of this assay.

20. Churcher, M.; Lamont, C.; Dingwall, C.; Green, S. M.; Lowe, A. D.; Butler, P. J. G.; Gait, M. J.; Karn, J. *J. Mol. Biol.* **1993**, *230*, 90.

21. (a) Smith, R. D.; Loo, J. A.; Edmonds, C. G.; Barinaga, C. J.; Udseth, H. R. *Anal. Chem.* **1990**, *62*, 882. (b) Ganem, B.; Henion, J. D. *Chemtracts-Org. Chem.* **1993**, *6*, 1. (c) Siuzdak, G. *Proc. Natl. Acad. Sci. U.S.A.* **1994**, *91*, 11290. (d) Loo, J. A. *Bioconj. Chem.* **1995**, *6*, 644.

22. Loo, J. A.; Sannes-Lowery, K. A.; Hu, P.; Mei, H.-Y.; Mack, D. P. *NATO ASI Series on New Methods for the Study of Molecular Aggregates*; Standing, K. G., Ed.; Kluwer, in press.

23. Moazed, D.; Noller, H. F. *Science* **1987**, *327*, 389.

24. Du, B.; Wu, P.; Boldt-Houle, D. M.; Terwilliger, E. F. *Gene Ther.* **1996**, *3*, 254.

25. Li, C. J.; Wang, C.; Pardee, A. B. *J. Biol. Chem.* **1994**, *269*, 7051.

26. (a) Ensoli, B.; Gendelman, R.; Markham, P.; Fiorelli, V.; Colombini, S.; Raffeld, M.; Cafaro, A.; Chang, H.-K.; Brady, J. N.; Gallo, R. C. *Nature (London)* **1995**, *371*, 674. (b) Milani, D.; Mazzoni, M.; Borgatti, P.; Zauli, G.; Cantley, L.; Capitani, S. *J. Biol. Chem.* **1996**, *271*, 22961. (c) Sastry, K. J.; Marin, M. C.; Nehete, P. N.; McConnell, K.; El-Naggar, A. K.; McDonnell, T. J. *Oncogene* **1996**, *13*, 487.

27. (a) Stewart, J. M.; Young, J. D. In *Solid Phase Peptide Synthesis, 2nd ed.*; Pierce Chemical: Rockford, 1984. (b) Bodansky, M.; Bodansky, A. In *The Practice of Peptide Synthesis*; Springer: Berlin, 1984.

28. Frankel, A. D.; Bredt, D. S.; Pabo, C. O. *Science* **1988**, *240*, 70.

29. Applied Biosystems User Bulletin No. 53. RNA Synthesis with DMT-cyanoethyl RNA Phosphoramidites.

(*Received in U.S.A.* 29 *October* 1996; *accepted* 18 *February* 1997)